

ResKD: Residual-Guided Knowledge Distillation

Xuwei Li*, Songyuan Li*, Bourahla Omar, Fei Wu, and Xi Li

Abstract—Knowledge distillation, aimed at transferring the knowledge from a heavy teacher network to a lightweight student network, has emerged as a promising technique for compressing neural networks. However, due to the capacity gap between the heavy teacher and the lightweight student, there still exists a significant performance gap between them. In this paper, we see knowledge distillation in a fresh light, using the knowledge gap, or the *residual*, between a teacher and a student as guidance to train a much more lightweight student, called a res-student. We combine the student and the res-student into a new student, where the res-student rectifies the errors of the former student. Such a residual-guided process can be repeated until the user strikes the balance between accuracy and cost. At inference time, we propose a sample-adaptive strategy to decide which res-students are not necessary for each sample, which can save computational cost. Experimental results show that we achieve competitive performance with 18.04%, 23.14%, 53.59%, and 56.86% of the teachers’ computational costs on the CIFAR-10, CIFAR-100, Tiny-ImageNet, and ImageNet datasets. Finally, we do thorough theoretical and empirical analysis for our method.

Index Terms—Knowledge Distillation, Residual, Sample-Adaptive.

I. INTRODUCTION

AS deep learning goes deeper, state-of-the-art neural networks [1], [2], [3], [4] have obtained better and better performance, and yet demand more and more computational resources. While models with large capacity can achieve high accuracy, they are impractical for resource-limited devices such as embedded systems. To this end, researchers have studied cost-effective networks [5], [6], [7], [8] and efficient training strategies [9], [10], [11], [12], [13], [14], [15], [16], [17]. Knowledge distillation (KD) [18] has emerged as a compression technique where an analogy of the teacher-student relationship is drawn to explain the idea that the knowledge of a powerful yet heavy teacher network can be distilled into a lightweight student network by adding a loss term that encourages the student to mimic the teacher.

Due to the capacity gap between a heavy teacher and a lightweight student, there is still a significant performance gap between them. Existing KD methods have made efforts to modify the loss term to improve the student’s performance [9], [19], [20], [21], [22]. However, the discrepancy between a teacher and a student can be considered as knowledge, and it remains relatively unexplored in knowledge distillation.

In this paper, we see knowledge distillation in a fresh light, using the knowledge gap between a teacher and a student as guidance. First, we train a student network S_0 from a teacher T as usual. Then, we train a much more lightweight

network, named a res-student, to learn the knowledge gap, or the *residual*, between the teacher T and the student S_0 . The combination of the student S_0 and the res-student R_1 becomes a new student S_1 , where R_1 corrects the errors of S_0 . Similarly, an even more lightweight res-student R_2 can be used to learn the knowledge gap between T and S_1 to build a new student S_2 . Such a residual-guided process can be repeated until a final student S_n is obtained. We call our framework residual-guided knowledge distillation (ResKD). The idea is akin to approximating functions by a polynomial. In a series expansion of a function, a higher-order polynomial would be a better approximation but would demand more computations. Similarly, a higher-order ResKD-style student would be closer to the teacher but would be more expensive. Users can control the total capacity of the final student network S_n by setting hyper-parameters for termination.

In addition, the knowledge gap mentioned above is different from sample to sample. For instance, given an S_2 student, we observed that, for some images, S_1 (i.e., $S_0 + R_1$) or even S_0 itself has highly confident scores, while R_2 or $R_1 + R_2$ has little contributions. It is unnecessary to use all the res-students for each sample at inference time. Thus, we introduce a sample-adaptive strategy for the inference phase. For each sample, if the confidence of S_i is high enough, we truncate the unnecessary res-students to save computational cost.

We do experiments on several standard benchmarks. The experimental results show that we achieve competitive performance with 18.04%, 23.14%, 53.59%, and 56.86% of the teacher’s FLOPs for CIFAR-10, CIFAR-100, Tiny-ImageNet, and ImageNet respectively. Also, we apply our ResKD framework to different KD methods and show that the framework is generic to knowledge distillation methods. Finally, we analyze the effectiveness of this idea and use informativeness [23] to visualize the bridging gap process.

Our contributions in this paper are summarized as follows:

- We design a residual-guided learning method that uses a series of res-students to bridge the gap between a student network and a teacher network.
- We introduce a sample-adaptive strategy at inference time to make our framework adaptive to different samples to save the cost of additional res-student networks.
- We evaluate our method on different datasets and perform detailed experiments that showcase the importance of each part of the framework.

II. RELATED WORK

A. Knowledge Distillation

We categorize knowledge distillation methods in terms of the number of stages. Traditionally, knowledge distillation is a two-stage method, in which a teacher network is trained first,

X. Li, S. Li, B. Omar, F. Wu and X. Li are with College of Computer Science and Technology, Zhejiang University, Hangzhou 310027, China. E-mail: {3150104097, leizungjun, bourahla, xilizju}@zju.edu.cn.

The first two authors (Xuwei Li and Songyuan Li) contribute equally. (Corresponding author: Xi Li.)

and then a student network is trained under the guidance of the teacher network. Bucilă et al. [24] pioneered the idea of transferring the knowledge from a cumbersome model to a small model. Hinton et al. [18] popularized this idea by the concept of knowledge distillation (KD), in which a student neural network is trained with the benefit of the soft targets provided by teacher networks. Compared to traditional one-hot labels, the output from a teacher network contains more information about the fine-grained distribution of data, which helps the student achieve better performance. Recently, many works have focused on improving the information propagation way or putting strictness to the distillation process via optimization [25], [26], [27], [19], [28], [29], [30], [31], [32], [33], [34], [35], [36], [37] to teach the student better. For example, Peng et al. [19] proposed that a student network should not only focus on mimicking from a teacher at an instance level, but also imitating the embedding space of a teacher so that the student can possess intra-class compactness and inter-class separability. In addition, the effect of different teachers is also researched [38], [39], [40]. For example, Sau et al. [39] proposed an approach to simulate the effect of multiple teachers by injecting noise to the training data and perturbing the logit outputs of a teacher. In such a way, the perturbed outputs not only simulate the setting of multiple teachers but also result in noise in the softmax layer, thus regularizing the distillation loss. With the help of many teachers, the student is improved a lot. Kang et al. [40] used Neural Architecture Search (NAS) to acquire knowledge for both the architecture and the parameters of the student network from different teachers. Besides the classic image classification task, KD can also be used in many other different fields, such as face recognition [41], visual question answering [42], video tasks [43], [44] etc.

Recently, some KD methods have been proposed to have less or more than two stages. For one thing, KD can be a one-stage strategy [45], [9]. Zhang et al. [9] proposed that a pool of untrained student networks with the same network structure can be used to simultaneously learn the target task together instead of the traditional two-stage knowledge distillation strategy. For another, a line of research [46], [47] focuses on KD methods with more than two stages. In [46], several Teacher Assistant networks are used to transfer the knowledge from a teacher more softly and effectively. The teacher propagates its knowledge to the assistant networks first and then the assistant networks propagate its knowledge to the student network. In [47], the student network has the same architecture as the teacher network at the beginning. The last block of the student network is replaced by a simple block and trained at the first stage. Next, the penultimate block is replaced similarly and the last two blocks are trained. In this style, all blocks are trained after several stages and a lightweight student network is achieved in the end.

In this paper, we mainly focus on how to use the gap between the teacher and the student as knowledge. We use a series of lightweight networks, named res-students, to learn the gap in a multi-stage manner.

B. Ensemble Methods

Ensemble methods, which have been studied extensively for improving model performance [48], [49], [50], are strategies to combine models by averaging, majority voting or something else, which means several models having the same status are used to improving final performance. Ensembles of models perform at least as well as each of its ensemble members [51]. There are several lines of research of ensemble methods: introducing different regularization, reducing training time [52] and saving test time [24].

For combining knowledge distillation and the ensemble idea, Lan et al. [53] proposed to aggregate the logits of several homogeneous student models to become an ensemble teacher and then to distill the knowledge from the teacher. On the contrary, we first carry on knowledge distillation to build a student and res-students and then combine them. Also, the roles that the student and res-students play are not the same. The student acquires the knowledge from the teacher, while the res-students acquire the knowledge from knowledge gaps. Furthermore, we introduce a sample-adaptive strategy to decide which res-students to use at inference time.

C. Residual Learning

Residual learning has been studied in face alignment for improving the final performance by learning from the gap between the suboptimal results and the target. Specifically, regressors for face alignment refine the current suboptimal results (landmark [54], [55], [56], [57], shape estimation [58] or heatmaps [59]) to approach the target. In [56], local binary features are extracted first and then a learning global linear regression is applied to generate the final landmark. In [58], a cascade shape regression are employed to generate the optimal pose from the initial pose according to the shape-indexed features of the input image. In [59], heatmaps and suboptimal landmarks are extracted by a multi-order cross geometry-aware model from the original images and a multi-order high-precision hourglass network is applied to achieve the heatmap subpixel face alignment and generate the optimal landmarks.

Knowledge distillation aims to deliver a lightweight student network to approximate a given teacher network. At training time, our ResKD learns not only from the ground truth but also from the residual between the teacher network and the former student network in a coarse-to-fine manner. When learning from the teacher network, our residual-guided supervision can be applied at different levels: the final output (just as the ground truth), intermediate feature maps, structural knowledge, etc.

III. RESIDUAL-GUIDED KNOWLEDGE DISTILLATION

In this section, we present our residual-guided knowledge distillation framework (ResKD). First, we briefly introduce the background. Second, we describe our main idea of residual-guided learning. Next, we propose a sample-adaptive strategy at inference time. Finally, we put all the things together to build a whole framework. For convenience, Table I summarizes the notations we use in this section.

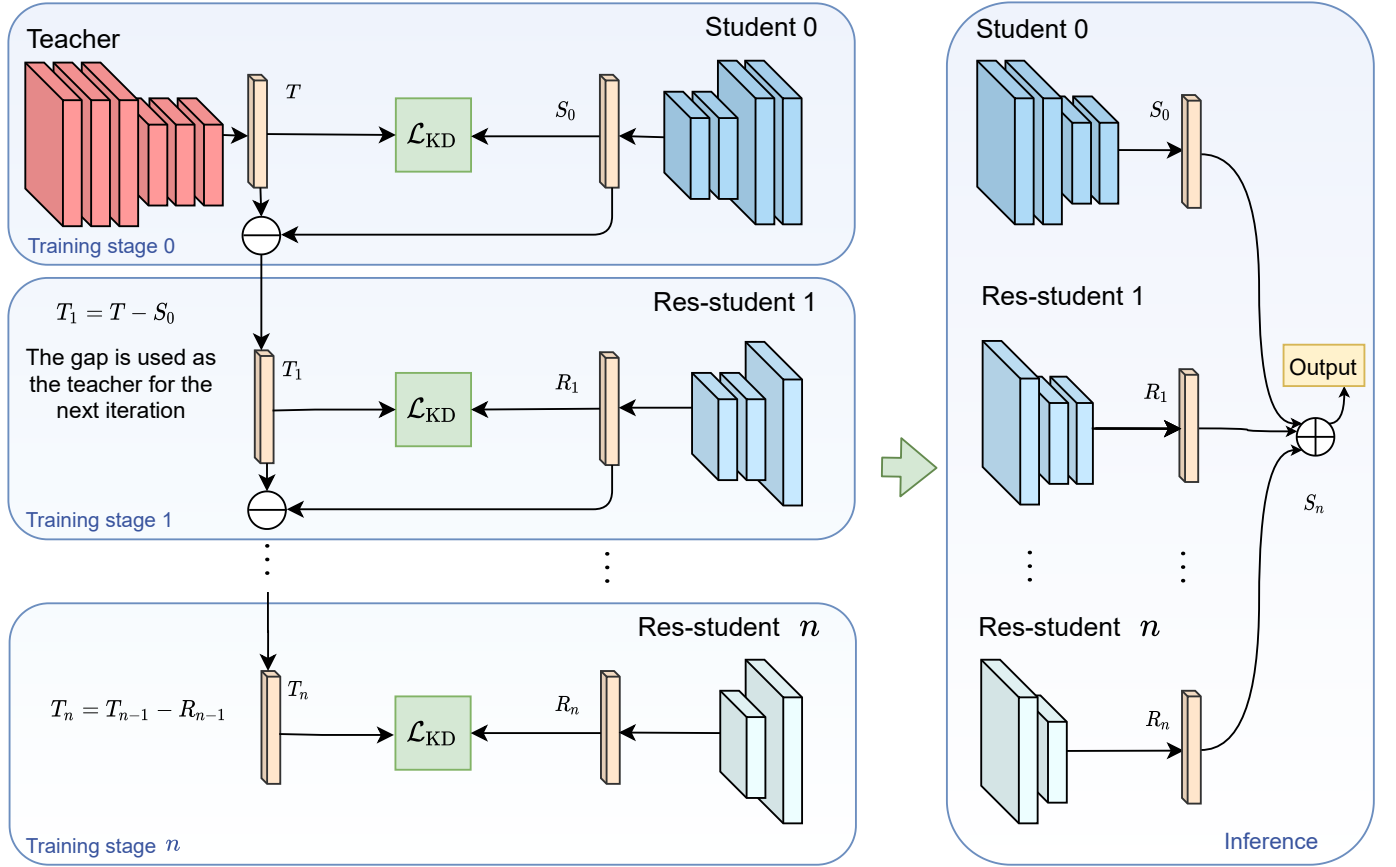


Fig. 1: (Best viewed in color) The main idea of the ResKD framework. Training stage 0 is just the same as traditional KD: a student network S_0 is trained to learn from a teacher T . In stage 1, a res-student R_1 is trained to learn from a teacher T_1 which is the residual between T and S_0 . Similarly, in stage i , a res-student R_i is trained from a teacher T_i until R_n is obtained. S_0 and all the res-students are combined to build a new student S_n .

TABLE I: Notations

T	A teacher network or its logits
S_0	A classic student network or its logits
$S_i, i > 0$	A ResKD student network or its logits
R_i	A res-student network or its logits
Δ_0	The gap between S_0 and T
$\Delta_i, i > 0$	The gap between S_i and T_i
D_t	A training set
D_v	A validation set
\mathcal{L}_{KD}	The knowledge distillation loss function
\mathcal{L}_{T-S}	The loss function used between logits of T and S
$\sigma(\cdot)$	The Softmax function
\mathbf{f}_j	Feature maps

A. Background and Notations

We first describe a general formulation of knowledge distillation, and then introduce the residual-guided knowledge distillation in this formulation.

We define a teacher network T as a function

$$T = f(\mathbf{x}, w_T, \alpha_T), \quad (1)$$

where \mathbf{x} is an input image, w_T is the weights of T , and α_T is its architecture parameters. Similarly, $S = f(\mathbf{x}, w_S, \alpha_S)$ denotes a student network. For convenience, a network and its logits are used interchangeably. The goal of knowledge distillation is to

learn w_S so that the results of the student S are as close as possible to the teacher T .

Classic knowledge distillation from a teacher is done in two steps. First, the student architecture α_S is determined. Then, w_S is optimized by

$$\argmin_{w_S} \sum_{j=1}^N \mathcal{L}_{KD} \left(f(\mathbf{x}^{(j)}, w_S, \alpha_S), f(\mathbf{x}^{(j)}, w_T, \alpha_T) \right), \quad (2)$$

where $\mathbf{x}^{(j)}$ is an input image in a dataset with N training samples and \mathcal{L}_{KD} is defined as

$$\mathcal{L}_{KD}(S, y^{(j)}, T, \tau, t) = \tau \cdot t^2 \cdot \mathcal{L}_{T-S}(\sigma(\frac{S}{t}), \sigma(\frac{T}{t})) + (1 - \tau) \cdot \mathcal{L}_{CE}(\sigma(S), y^{(j)}), \quad (3)$$

where $y^{(j)}$ is the label of the input image $\mathbf{x}^{(j)}$, $\sigma(\cdot)$ is the softmax function, \mathcal{L}_{CE} is the conventional cross-entropy loss function, τ and t are scalar hyper-parameters, and \mathcal{L}_{T-S} is the loss between the student's logits and the teacher's logits, e.g., the Kullback–Leibler divergence.

The optimized w_S from Eq. (2) makes the predictions obtained from $S = f(\mathbf{x}, w_S, \alpha_S)$ as close to those obtained by

$T = f(\mathbf{x}, w_T, \alpha_T)$ as possible, but we still observe a difference Δ between the teacher's and student's logits:

$$\Delta = T - S, \quad (4)$$

which is what we propose to reduce as follows.

B. Residual-Guided Learning

We propose a framework distilling knowledge in a residual-guided fashion: we use the difference, or the *residual*, between a teacher and a student as guidance. Given a teacher network, we first train a student network by classic knowledge distillation. Then, we introduce another student, called a res-student, to learn their residual. After that, we combine the original student and the res-student to form a new student. Such a process can be repeated to add more res-students to further bridge the performance gap, as shown in Fig. 1.

Formally, let the logits of the teacher be T , the logits of the first student be S_0 , and the logits of the res-student networks be $\{R_i\}_{i=1}^n$. We train S_0 and $\{R_i\}_{i=1}^n$ in stages. In stage 0, S_0 is trained in a classic knowledge distillation manner with T as the teacher network. The gap can be observed by $\Delta_0 = T - S_0$. In stage 1, the gap Δ_0 is defined as a new teacher, i.e., $T_1 = \Delta_0$, to train a res-student R_1 . Once we obtain R_1 , we can define a new student $S_1 = S_0 + R_1$. Similarly, in each following stage, we use the gap from the current stage $\Delta_i = T_i - R_i$ as the next stage teacher network T_{i+1} . We distill a res-student R_{i+1} from T_{i+1} and obtain the next student $S_{i+1} = S_0 + R_1 + \dots + R_{i+1}$. Finally, we use the student network and res-student networks trained in all $n + 1$ stages. We feed an input image to all networks independently and sum their logits to obtain the final logits:

$$S_n = S_0 + \sum_{i=1}^n R_i. \quad (5)$$

1) *NAS-Assisted Architecture*: When we use a res-student to bridge the gap to the teacher, it is better to use NAS to get the architecture of the res-student network instead of a handcrafted one. We also use the knowledge distillation loss function in the search stage when using NAS, which is reflected by adding α_S as an optimizable parameter in Eq. (2):

$$\operatorname{argmin}_{w_S, \alpha_S} \sum_{j=1}^N \mathcal{L}_{\text{KD}} \left(f(\mathbf{x}^{(j)}, w_S, \alpha_S), f(\mathbf{x}^{(j)}, w_T, \alpha_T) \right). \quad (6)$$

We use the same search space as that of STACNAS [60]. A STACNAS-style neural network consists of a series of building blocks called cells. We define a set of candidate operations O to be used inside these cells, and from which we will select the best operations for the architecture.

The construction of cells and the whole network can be described as a directed acyclic graph (DAG) as shown in Fig. 2. A cell contains a sequence of N nodes $\mathbf{f}_1, \mathbf{f}_2, \dots, \mathbf{f}_N$ each of which is a stack of feature maps. These nodes are connected by directed edges. An edge (i, j) represents some operation $o_k^{(i,j)}(\cdot) \in O$ that transforms \mathbf{f}_i to \mathbf{f}_j . In a certain cell, each node is computed as a weighted sum of all its predecessors:

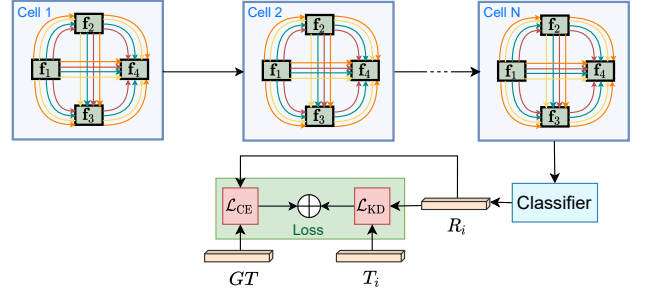


Fig. 2: The overview of our NAS-assisted architecture. We use the same setting as that of STACNAS[60]. In addition, we use KD loss in both search and fine-tuning stages.

$$\mathbf{f}_j = \sum_{i < j} \sum_{o_k \in O} \alpha_k^{(i,j)} o_k^{(i,j)}(\mathbf{f}_i), \quad (7)$$

where $\alpha_k^{(i,j)}$ is the weight for the operation $o_k^{(i,j)}$ applied to \mathbf{f}_i when calculating the node \mathbf{f}_j . We use the same training strategy as that of STACNAS [60] to obtain the final suitable network.

2) *Termination Condition*: When a ResKD student S_i is close enough to the teacher T , we can stop the residual-guided process. Here, we define a concept “Energy” to measure the difference between a student and a teacher.

The Energy of network S_i for a certain sample $\mathbf{x}^{(j)}$ is

$$\text{Energy}(S_i, \{\mathbf{x}^{(j)}\}) = \|\sigma(S_i(\mathbf{x}^{(j)}))\|_2^2, \quad (8)$$

where $\sigma(\cdot)$ is the softmax function, and thus the Energy of network S_i on dataset D is

$$\text{Energy}(S_i, D) = \frac{1}{N} \cdot \sum_{j=1}^N \|\sigma(S_i(\mathbf{x}^{(j)}))\|_2^2, \quad (9)$$

where N is the total number of samples in dataset D . In this way, the Energy of a network represents its overall confidence on a dataset. When the Energy of S_i has reached a comparable level of the Teacher’s Energy (e.g., 90%), we can set $n = i$ and finish the residual-guided learning process.

In practice, we calculate Energy on a validation set D_v whose data are uniformly sampled from the training set D . The overall training process is shown in Algorithm 1.

C. Sample-Adaptive Inference

When we finish the residual-guided learning process, we have $S_n = S_0 + \sum_{i=1}^n R_i$, where R_i is supposed to bridge the gap Δ_{i-1} between S_{i-1} and T . However, for each sample, Δ_{i-1} is also different. For instance, if the sample is easy to recognize, Δ_0 can be subtle, and if the sample is difficult, even Δ_2 can be considerable. In other words, for an easy sample, S_0 is enough, but for a difficult sample, we should use more res-students.

Based on the above observation, we propose an adaptive strategy for each sample at inference time. Similar to the Energy idea in Section III-B, we uniformly sample a validation

Algorithm 1 ResKD training

Input: Training set $D_t = \{(\mathbf{x}^{(j)}, y^{(j)})\}_{j=1}^N$ and teacher network $T(\mathbf{x}) = f(\mathbf{x}, w_T, \alpha_T)$.
Output: $S_0, R_1, R_2, \dots, R_n$ and a threshold $\text{TH}_{\text{energy}}$.
 Sample a validation set $D_v = \{(\mathbf{x}^{(j)}, y^{(j)})\}_{j=1}^{N_v}$ from the training set D_t uniformly.
 Train S_0 ; $T_1 = \Delta_0 = T - S_0$; $i = 0$.
repeat
 $i = i + 1$.
 $R_i = \text{KD}(T_i)$.
 $T_{i+1} = T_i - R_i$; $S_i = S_{i-1} + R_i$.
until $\text{Energy}(S_i, D_v) > 90\% \cdot \text{Energy}(T, D_v)$
 $n = i$.
 $\text{TH}_{\text{energy}} = \text{Energy}(S_n, D_v)$
return networks S_0, R_1, \dots, R_n and a threshold $\text{TH}_{\text{energy}}$.

set D_v from the training set D , and calculate an Energy threshold for the final ResKD student S_n :

$$\text{TH}_{\text{energy}} = \text{Energy}(S_n, D_v). \quad (10)$$

When the Energy of S_i with a sample $\mathbf{x}^{(j)}$, i.e., $\text{Energy}(S_i, \{\mathbf{x}^{(j)}\})$, is higher than $\text{TH}_{\text{energy}}$, we set the rest res-students R_{i+1}, \dots, R_n aside. As a result, given a sample $\mathbf{x}^{(j)}$, we define $S_n^{(i)}$ as the student network it uses at inference time:

$$S_n^{(i)}(\mathbf{x}^{(j)}) = S_L(\mathbf{x}^{(j)}), \quad 0 \leq L \leq n, \quad (11)$$

where we use S_L instead of S_n for the sample $\mathbf{x}^{(j)}$. For example, let $S_n = S_3$. Given a sample $\mathbf{x}^{(j)}$, if $\text{Energy}(S_1, \mathbf{x}^{(j)}) > \text{TH}_{\text{energy}}$, then $L = 1$, which means that we only use S_0 and R_1 , and set R_2 and R_3 aside. The whole process is shown in Algorithm 2.

D. ResKD: The Whole Framework

When faced with a knowledge distillation problem, our first step is to train a student network S_0 , which can be handcrafted or searched, under the guidance of the teacher T . Next, we start to use our residual-guided learning strategy to find res-students. We train the res-student R_i in a KD manner under the guidance of T_i . Such a residual-guided process can be repeated until S_i has achieved the Energy comparable to T . At inference time, we apply our sample-adaptive strategy.

IV. EXPERIMENTS

In this section, we first introduce the datasets and protocols we use in Section IV-A. Next, we do ablation studies in Section IV-B1 and Section IV-B2 to evaluate the effectiveness of our strategies. Finally, we evaluate our framework on several datasets in Section IV-B3.

A. Datasets and Protocols

1) *CIFAR-10/100*: The CIFAR-10/100 dataset consists of 50k training images and 10k testing images in 10/100 classes. We use a weight decay of 0.0001 and a momentum of 0.9. Our

Algorithm 2 Sample-adaptive inference

Input: a test sample $\mathbf{x}^{(j)}$, networks $S_0, R_1, R_2, \dots, R_n$ and a threshold $\text{TH}_{\text{energy}}$.
Output: S_L and the logits of S_L for the test sample $\mathbf{x}^{(j)}$.
 calculate $S_0(\mathbf{x}^{(j)})$; $E_0 = \text{Energy}(S_0, \{\mathbf{x}^{(j)}\})$.
 $i = 0$.
while $\text{TH}_{\text{energy}} \geq E_i$ and $i < n$. **do**
 calculate $R_i(\mathbf{x}^{(j)})$; $i = i + 1$
 $E_i = E_{i-1} + \text{Energy}(R_i, \{\mathbf{x}^{(j)}\})$.
end while
 $L = i$.
return S_L and the logits of S_L for the test sample $\mathbf{x}^{(j)}$.

models are trained with a mini-batch size of 128. We start with a learning rate of 0.1, divide it by 10 at 150 and 200 epochs, and terminate training at 250 epochs. We follow the simple data augmentation in [1] for training: 4 pixels are padded on each side, and a 32×32 crop is randomly sampled from the padded image or its horizontal flip for training. For testing, we only evaluate the single view of the original 32×32 image.

2) *ImageNet*: ImageNet consists of 1000 classes. Our models are trained on the 1.28 million training images, and evaluated on the 50k validation images. Images are randomly resized and a 224×224 crop is randomly sampled from the resized image or its horizontal flip for training. For testing, we scale the short side of images to 224, and a 224×224 center crop is sampled from the scaled image. When training ResNet series networks, We start with a learning rate of 0.1, divide it by 10 at 30, 60 and 80 epochs, and terminate training at 90 epochs. We use a weight decay of 0.0001 and a momentum of 0.9. When dealing with the network given by neural architecture search, we use a weight decay of 0.0003 and a momentum of 0.9. An exponential learning rate strategy is used to control the learning rate from 0.1 and multiplying the learning rate by 0.92 after each epoch. We use 100 epochs in total. Our models are trained with a mini-batch size of 128.

3) *Tiny-ImageNet*: Tiny-ImageNet consists of 200 classes. Our models are trained on the 100k training images, and evaluated on the 10k validation images. Images are randomly resized and a 224×224 crop is randomly sampled from the resized image or its horizontal flip for training. For testing, we resize the original images to 224×224 and evaluate them. When training ResNet series networks, we start with a learning rate of 0.1, divide it by 10 at 40, 80, and 120 epochs, and terminate training at 150 epochs. We use a weight decay of 0.0001 and momentum of 0.9. When dealing with the network given by neural architecture search, we use the same setting as we do on ImageNet. Our models are trained with a mini-batch size of 128.

When it comes to the termination condition of residual-guided learning, we set comparable Energy as 90% of T 's Energy. In the following sections, when it is not mentioned, we use L_2 loss function for the \mathcal{L}_{T-S} in Eq. (3). “KD” in some tables (e.g., Table VI) means using this loss function, too.

We do all experiments on four NVIDIA GTX 1080 Ti cards.

TABLE II: Comparison with other ensemble methods on CIFAR-10/100. Res110 is the ResNet-110 teacher network. Res20 (SGD) is a ResNet-20 trained with SGD, and Res20 (KD) is a ResNet-20 trained by KD to learn from the teacher. ‘Ensemble’, ‘Trained together’ and ‘Ours’ share the same architecture where S_0 is ResNet-20 and R_1 is ResNet-14. ‘Ensemble’ means that ResNet-20 and ResNet-14 are trained independently and the sum of their logits is used for evaluation. ‘Trained together’ means that the combination of ResNet-20 and ResNet-14 is trained together.

Architecture	Acc. (%)	#Params (M)	MFLOPs
<i>Teacher</i>			
Res110	94.19 / 72.44	1.728 / 1.734	255 / 255
<i>Students</i>			
Res20 (SGD)	91.80 / 68.82	0.270 / 0.276	41 / 41
Res20 (KD)	93.06 / 70.09	0.270 / 0.276	41 / 41
<i>Res20-14</i>			
ensemble	93.17 / 70.41	0.442 / 0.454	68 / 68
trained together	93.12 / 70.85	0.442 / 0.454	68 / 68
Ours	93.27 / 71.96	0.442 / 0.454	68 / 68

TABLE III: Multi-stage residual-guided learning on CIFAR-10/100. ResX-Y-Z means we use ResNet-X as S_0 , ResNet-Y as R_1 , and ResNet-Z as R_2 . Multi-stage residual-guided learning can further bridge the gap between the teacher and the student. **Bold**: The best results out of students. Underline: The second best results out of students.

Architecture	Acc. (%)	#Params (M)	MFLOPs
<i>Teacher</i>			
Res110	94.19 / 72.44	1.728 / 1.734	255 / 255
<i>Students</i>			
Res20 (SGD)	91.80 / 68.82	0.270 / 0.276	41 / 41
Res20 (KD)	93.06 / 70.09	0.270 / 0.276	41 / 41
<i>ResKD S_1</i>			
Res20-14	93.27 / 71.96	0.442 / 0.454	68 / 68
Res20-20	<u>93.35 / 72.22</u>	0.539 / 0.551	<u>82 / 82</u>
<i>ResKD S_2</i>			
Res20-14-8	93.30 / 72.18	0.518 / 0.535	80 / 80
Res20-14-14	93.68 / 72.42	0.615 / 0.632	94 / 94

B. Ablation Study

1) *Residual-Guided Learning*: First, we validate the effect of a res-student. We use ResNet-110 as the teacher T , ResNet-20 as the classic KD student S_0 , and ResNet-14 as the res-student R_1 . As illustrated in Table II, our ResKD student $S_1 = S_0 + R_1$ outperforms S_0 , which means a res-student can correct the errors of a classic KD student.

However, since we obtain a ResKD student by combining two networks, it is arguable whether the effect of the res-student comes from our residual-guided learning. It could be attributed to additional capacity. Thus, it is necessary to compare a ResKD student with other types of combinations, such as an ensemble network, to show the effect of our method. As illustrated in Table II, our method also outperforms the “ensemble” and the “trained together” approaches, which means that using res-students is more effective than using an

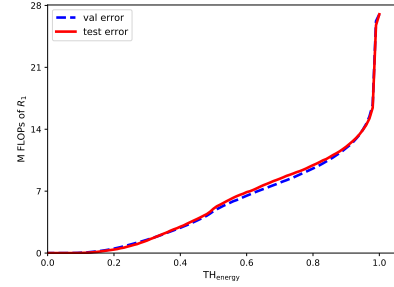


Fig. 3: The relationship between the cost reduction of R_1 and TH_{energy} on both validation set and test set on CIFAR-100. T is ResNet-110, S_0 is ResNet-20, and R_1 is ResNet-14. The result indicates that it is reasonable to calculate TH_{energy} on a validation set for the sample-adaptive strategy.

ensemble.

We can repeat residual-guided learning to further bridge the gap between the student and the teacher. As illustrated in Table III, we train another res-student R_2 to build S_2 , and the performance of S_2 is better than S_1 .

2) *Sample-Adaptive Inference*: This strategy focuses on striking the balance between performance and cost. Our threshold TH_{energy} based on the validation set is a key hyper-parameter in it. We justify our choice of TH_{energy} in two fields: our TH_{energy} can be generalized to the test set, and the TH_{energy} is effective.

Our sample-adaptive strategy focuses on striking the balance between performance and cost by setting TH_{energy} . According to the relationship between performance and cost w.r.t. TH_{energy} as shown in Fig. 4, we can set an appropriate TH_{energy} . We set TH_{energy} as 90% of the final student network’s energy (here is S_1 ’s energy) on the validation set to have a good trade-off. As a result, TH_{energy} is 0.88 for CIFAR-100 and 0.70 for ImageNet. In this case, our sample-adaptive strategy can avoid remarkable FLOPs of R_1 and preserve the accuracy at the same time.

We also verify the transfer from our validation set to the test set. We carry out experiments to show the relationship between TH_{energy} and cost on the validation and test set in Fig. 3. We can learn that as the TH_{energy} reduces, the decreasing styles of R_1 ’s cost on both settings are similar, which means the TH_{energy} based on the validation set is reasonable to use on the test set.

3) *The Whole Framework, ResKD*: We use our whole framework on CIFAR-10, CIFAR-100, Tiny-ImageNet and ImageNet. As illustrated in Table IV and Table V, ResKD achieves consistent results on these datasets. Our ResKD student $S_1 = S_0 + R_1$ where R_1 ’s architecture is searched by NAS outperforms S_0 in both accuracy and energy, which means a res-student can also correct the errors of a classic KD student on all four datasets.

C. Discussion

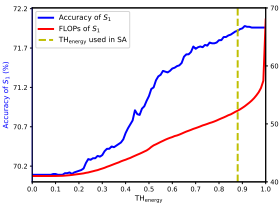
To verify the generalization of our ResKD, we carry out the following four case studies.

TABLE IV: Performance on CIFAR-10 / CIFAR-100. T is ResNet-110, S_0 is a ResNet-20, R_1 is a res-student whose architecture is searched by NAS. S_1 means using both S_0 and R_1 . ‘SA’ means using our sample-adaptive strategy at inference time. Energy is the metric we mention in Section III-B. **Bold**: The best results out of students. Underline: The second best results out of students.

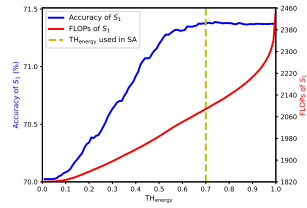
Architecture	Optimizer	SA	Acc. (%)	#Params (M)	MFLOPs	MFLOPs proportion to T (%)	Energy
<i>Teacher</i> Res110	SGD		94.19 / 72.44	1.728 / 1.734	255 / 255	100 / 100	0.9993 / 0.9894
<i>Students</i> S_0	KD		<u>93.06</u> / <u>70.09</u>	0.270 / 0.276	41 / 41	16.08 / 16.08	0.9923 / 0.8380
<i>ResKD students</i> S_1	KD		93.92 / 74.06	0.453 / 0.485	79 / 81	30.98 / 31.76	0.9958 / 0.9204
S_1	KD	✓	93.92 / 74.06	0.453 / 0.485	46 / 59	<u>18.04</u> / <u>23.14</u>	-

TABLE V: Performance on Tiny-ImageNet / ImageNet. T is ResNet-50, S_0 is a ResNet-18, R_1 is a res-student whose architecture is searched by NAS. S_1 means using both S_0 and R_1 . ‘SA’ means using our sample-adaptive strategy at inference time. Energy is the metric we mention in Section III-B. **Bold**: The best results out of students. Underline: The second best results out of students.

Architecture	Optimizer	SA	Acc. (%)	#Params (M)	MFLOPs	MFLOPs proportion to T (%)	Energy
<i>Teacher</i> Res50	SGD		70.42 / 75.50	23.92 / 25.56	4117 / 4119	100 / 100	0.9963 / 0.7782
<i>Students</i> S_0	KD		67.90 / 70.02	11.28 / 11.69	1821 / 1821	44.23 / 44.22	0.9805 / 0.6575
<i>ResKD students</i> S_1	KD		68.98 / 73.73	16.38 / 19.71	2453 / 2777	59.58 / 67.42	0.9919 / 0.8040
S_1	KD	✓	68.99 / <u>73.70</u>	16.38 / 19.71	2206 / 2342	<u>53.59</u> / <u>56.86</u>	-



(a) S_1 's accuracy and FLOPs with different TH_{energy} on CIFAR-100.



(b) S_1 's accuracy and FLOPs with different TH_{energy} on ImageNet.

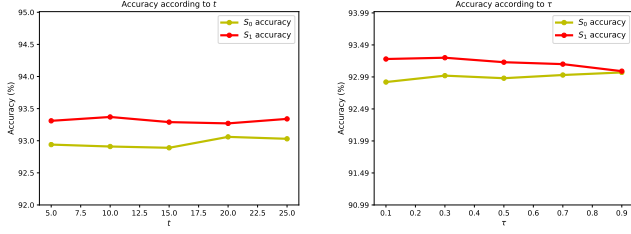
Fig. 4: This figure shows the results about TH_{energy} . (a) indicates the relationship between the performance and FLOPs of S_1 with different TH_{energy} on the test set on CIFAR-100. (b) shows the relationship on ImageNet. For CIFAR-100, T is ResNet-110, S_0 is ResNet-20, and R_1 is ResNet-14. For ImageNet, T is ResNet-50, S_0 is ResNet-18, and R_1 is a NAS-based architecture. The results indicate that our trade-off is done by our sample-adaptive strategy, and most of R_1 's FLOPs can be reduced with little performance decreasing.

1) *Different Loss Functions*: To show that our residual-guided learning is generic to different \mathcal{L}_{T-S} , we carry on experiments using Kullback–Leibler divergence and L_2 distance loss function on CIFAR-10. As illustrated in Table VI, both Kullback–Leibler divergence and L_2 distance loss function work well with our ResKD framework.

TABLE VI: The effect of different KD loss functions \mathcal{L}_{T-S} on CIFAR-10. ResX-Y-Z means we use ResNet-X as S_0 , ResNet-Y as R_1 , and ResNet-Z as R_2 . As a result, our framework is generic to \mathcal{L}_{T-S} . **Bold**: The best results out of students. Underline: The second best results out of students.

Architecture	Optimizer	\mathcal{L}_{KD}	Acc. (%)	#Params (M)	MFLOPs
<i>Teacher</i> Res110	SGD	-	94.19	1.728	255
<i>Students</i> Res20	SGD	-	91.80	0.270	41
Res20	KD	L_2	93.06	0.270	41
Res20	KD	KL	92.76	0.270	41
Res20	DML	L_2	92.53	0.270	41
Res20	RKD	L_2	92.45	0.270	41
<i>ResKD students</i> Res20-14	KD	L_2	93.27	0.442	68
Res20-14	KD	KL	93.50	0.442	<u>68</u>
Res20-20	KD	L_2	93.35	0.539	82
Res20-20	KD	KL	93.57	0.539	82
Res20-20-20	KD	L_2	93.95	0.809	123
Res20-20-20	KD	KL	93.93	0.809	123
Res20-14	DML	L_2	92.88	0.442	68
Res20-14	RKD	L_2	93.17	0.442	<u>68</u>

2) *Settings of τ and t* : We have tried different τ s (from 0.1 to 0.9) and t s (from 5 to 25) and choose the best one. It turns out that the performance of ResKD is not very sensitive to these hyper-parameter configurations as shown in Fig. 5. We set $\tau = 0.9/0.5/0.5/0.1$ for S_0 on CIFAR-10 / CIFAR-100 / Tiny-ImageNet / ImageNet, $\tau = 0.1$ for R_1 on all datasets and



(a) t 's influence on S_0 and S_1 . (b) τ 's influence on S_0 and S_1 .

Fig. 5: The relationship between hyper-parameters (τ and t) and the performance of S_0 and S_1 on CIFAR-10. T is ResNet-110, S_0 is ResNet-20, and R_1 is ResNet-14. The result indicates that these hyper-parameters can partly affect the final performance but not large.

TABLE VII: Performance on CIFAR-10 / CIFAR-100. R_1 is a res-student whose architecture is searched by NAS. The results of S_1 are combined with sample-adaptive inference. S_1 (VGG) / S_1 (Xception) / S_1 (Mobile) / S_1 (Shuffle) means S_0 is VGG11BN / Xception / MobileNetv2 / ShuffleNetv2 and R_1 is a NAS-based network. **Bold**: The best results out of students. Underline: The second best results out of students.

Architecture	Teacher	Acc. (%)	MFLOPs
Inceptionv3	-	95.28 / 79.40	3399 / 3400
Xception	-	94.58 / 78.13	1134 / 1134
Xception	Inceptionv3	94.99 / 78.58	1134 / 1134
S_1 (Xception)	Inceptionv3	96.15 / 83.13	1163 / 1394
VGG19BN	-	93.70 / 71.50	418 / 419
VGG11BN	-	91.99 / 68.96	172 / 173
VGG11BN	VGG19BN	92.17 / 71.46	172 / 173
S_1 (VGG)	VGG19BN	94.01 / 76.58	206 / 203
ResNet50	-	95.33 / 78.21	1305 / 1306
MobileNetv2	-	92.75 / 69.30	67 / 68
MobileNetv2	ResNet50	93.21 / 75.31	67 / 68
S_1 (Mobile)	ResNet50	93.83 / 78.30	70 / 101
ShuffleNetv2	-	93.40 / 71.52	45 / 46
ShuffleNetv2	ResNet50	93.98 / 75.92	45 / 46
S_1 (Shuffle)	ResNet50	94.56 / 78.57	<u>49</u> / <u>65</u>

$t = 20$ in all situations.

3) *Different Backbones*: To show that our framework is generic to different backbones, we also apply our residual-guided learning to other networks like VGG-11, MobileNetv2, ShuffleNetv2, and Xception. As shown in Table VII, our framework achieves consistent results with different backbones.

4) *Accuracy-Cost Trade-off*: We show the comparison of the accuracy-cost trade-off between ResKD and the baseline as illustrated in Fig. 6. With the same FLOPs, ResKD models achieve better accuracy, and when achieving the same accuracy, ResKD models demand less FLOPs.

5) *Different KD Methods*: To show that our ResKD framework is generic to other distillation methods (feature distillation and both prediction and feature distillation) and for a fair comparison, we use the new implementation [37]. Experimental results show that our ResKD models achieve consistent accuracy improvement for all the twelve KD methods as

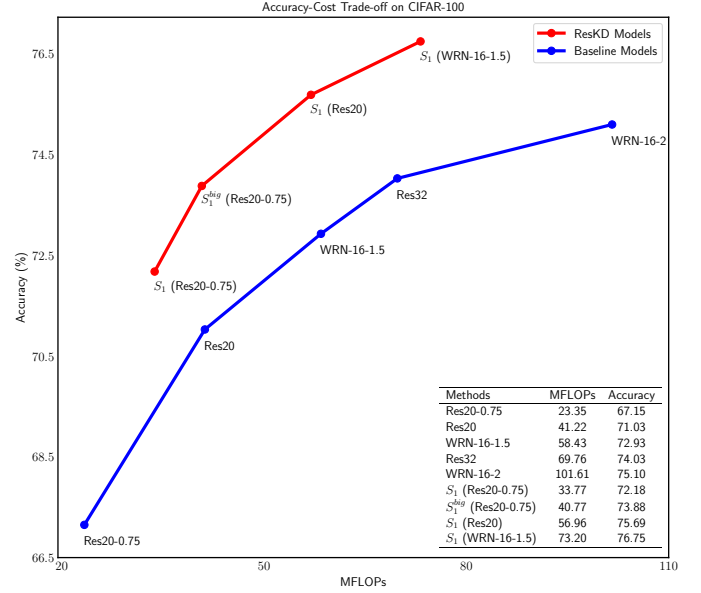


Fig. 6: Accuracy-cost trade-off on CIFAR-100. The blue line shows the accuracy-cost tendency of baseline models whereas the red line indicates the trend of ResKD models. “ S_1 (Res20)”: ResNet-20 is used as S_0 ; “ S_1 (Res20-0.75)”: the tailored ResNet-20 where the channel number of each layer is 75% of the original ResNet-20 is used as S_0 ; “WRN-16-2”: the wide residual network whose depth and widening factor is 16 and 2; S_1^{big} (Res20-0.75): similar to S_1 (Res20-0.75) but having a relatively big R_1 . We use the original knowledge distillation [18] in this experiment.

shown in Table VIII.

V. ANALYSIS: WHY RESIDUAL-GUIDED LEARNING WORKS

In this section, we try to shed some light on why and how our residual-guided learning helps the training process.

A. Theoretical Analysis

Our residual-guided learning is based on the gap between a teacher T and a student S . We should use a suitable metric to measure the gap between T and S . Many metrics are already proposed from simple L_1 , L_2 to complex metrics in [61], [23], [62], [63]. Inspired by [23], we measure the informativeness of training examples by analyzing their resulting gradients since the training data contribute to optimization via gradients. The gap of informativeness (gap_info, GI) between S and T for a training example $\mathbf{x}^{(j)}$ at an iteration t is defined as:

$$\text{GI}(\mathbf{x}^{(j)}, S, T, t) = \|\nabla_{\theta_t} \mathcal{L}(S(\mathbf{x}^{(j)}), T(\mathbf{x}^{(j)}))\|_2, \quad (12)$$

where ∇_{θ_t} denotes the gradients of S 's parameters θ at the iteration t . However, computing this L_2 -norm directly is expensive. Instead, we could estimate the upper bound $\widehat{\text{GI}}$ for GI.

TABLE VIII: The results of different distillation methods on CIFAR-100. T is ResNet-110 with an accuracy of 74.31% and a cost of 255.28 MFLOPs. S_0 is ResNet-20. S_1 is a NAS-based network R_1 combined with S_0 . We report the accuracies as “69.65 / 68.99 [37]”, which means that the re-implemented accuracy is 69.65, and the reported accuracy in [37] is 68.99. For a fair comparison, we control the cost of all S_1 at a similar level. Our ResKD can work well with different distillation methods.

KD Method	Model	Accuracy (%)	MFLOPs
<i>Feature Distillation</i>			
FitNet [25]	S_0	69.65 / 68.99 [37]	41.22
	S_1	75.12 (+5.47 / +6.13)	64.49 (+23.27)
AT [27]	S_0	70.50 / 70.22 [37]	41.22
	S_1	75.65 (+5.15 / +5.43)	63.74 (+22.52)
SP [28]	S_0	70.72 / 70.04 [37]	41.22
	S_1	75.44 (+4.72 / +5.40)	63.63 (+22.41)
CC [19]	S_0	69.44 / 69.48 [37]	41.22
	S_1	75.34 (+5.90 / +5.86)	65.72 (+24.50)
VID [32]	S_0	70.22 / 70.16 [37]	41.22
	S_1	76.10 (+5.88 / +5.94)	63.46 (+22.24)
RKD [30]	S_0	69.40 / 69.25 [37]	41.22
	S_1	75.52 (+6.12 / +6.27)	64.97 (+23.75)
PKT [34]	S_0	70.38 / 70.25 [37]	41.22
	S_1	75.82 (+5.44 / +5.57)	64.02 (+22.80)
AB [36]	S_0	69.94 / 69.53 [37]	41.22
	S_1	77.11 (+7.17 / +7.58)	64.75 (+23.53)
FT [35]	S_0	70.06 / 70.22 [37]	41.22
	S_1	75.78 (+5.72 / +5.56)	64.45 (+23.23)
NST [33]	S_0	70.24 / 69.53 [37]	41.22
	S_1	75.93 (+5.69 / +6.40)	64.46 (+23.24)
CRD [37]	S_0	71.33 / 71.46 [37]	41.22
	S_1	76.07 (+4.74 / +4.61)	62.80 (+21.58)
<i>Both Prediction and Feature Distillation</i>			
CRD+KD [37]	S_0	71.61 / 71.56 [37]	41.22
	S_1	75.75 (+4.14 / +4.19)	57.37 (+16.15)

Following the work of [64] and without loss of generality, we use a multi-layer perceptron (MLP) as the model in our analysis. Let $\theta^{(l)} \in \mathbb{R}^{M_l \times M_{l-1}}$ be the weight matrix for layer l and $\sigma^{(l)}(\cdot)$ be a Lipschitz continuous activation function, and then we have:

$$\begin{aligned}
 \mathbf{a}^{(0)} &= \mathbf{x}^{(j)}, \\
 h^{(l)} &= \theta^{(l)} \mathbf{a}^{(l-1)}, \\
 \mathbf{a}^{(l)} &= \sigma^{(l)}(h^{(l)}), \\
 f(\mathbf{x}^{(j)}, \theta) &= \mathbf{a}^{(L)},
 \end{aligned} \tag{13}$$

where $\mathbf{a}^{(l)}$ denotes the feature maps after layer l and $\mathbf{x}^{(j)}$ is a certain sample. We define:

$$\Sigma'_l(h^{(l)}) = \text{diag}(\sigma'^{(l)}(h_1^{(l)}), \sigma'^{(l)}(h_2^{(l)}) \dots, \sigma'^{(l)}(h_{M_l}^{(l)})). \tag{14}$$

$$\Pi^{(l)} = \left(\prod_{i=l}^{L-1} \Sigma'_i(h^{(i)}) \theta_{i+1}^T \right) \Sigma'_L(h^{(L)}). \tag{15}$$

TABLE IX: GI of different student networks to the teacher network on CIFAR-10. T is ResNet-110, and S_0 is ResNet-20. Res X - Y - Z means that we use ResNet- X as S_0 , ResNet- Y as R_1 , and ResNet- Z as R_2 . **Bold**: The best results out of students.

Architecture	Acc. (%)	L_2 to T	GI/ C_1 to T
<i>Teacher</i>			
Res110	94.19	-	-
<i>Student</i>			
Res20	93.06	0.90	1.73
<i>ResKD networks</i>			
Res20-8	93.03	0.82	1.64
Res20-14	93.27	0.74	1.53
Res20-20	93.35	0.61	1.37
Res20-20-8	93.55	0.49	1.15
Res20-20-14	93.84	0.43	1.03
Res20-20-20	93.95	0.37	0.89

\mathcal{L} is the loss function $\mathcal{L}(S(\mathbf{x}^{(i)}), T(\mathbf{x}^{(i)}))$ in Eq. (12). The $\text{GI}^{(l)}$ is the informativeness of the parameters in layer l and it can be expressed as:

$$\begin{aligned}
 \text{GI}^{(l)} &= \|(\Pi^{(l)} \nabla_{\mathbf{a}^{(L)}} \mathcal{L})(\mathbf{a}^{(l-1)})^T\|_2 \\
 &\leq \|\Pi^{(l)}\|_2 \|(\mathbf{a}^{(l-1)})^T\|_2 \|\nabla_{\mathbf{a}^{(L)}} \mathcal{L}\|_2.
 \end{aligned} \tag{16}$$

Various weight initialization [65] and activation normalization techniques [66], [67] uniformize the activations across samples. As a result, the variation of the gradient norm is mostly captured by the gradient of the loss function with respect to the pre-activation outputs of the last layer of our neural network. Consequently, we can derive the following upper bound to the gradient norm of all the parameters. Suppose that C_{max} is a constant:

$$\text{GI} \leq C_{max} \|\nabla_{\mathbf{a}^{(L)}} \mathcal{L}\|_2. \tag{17}$$

Based on Eq. (17), we set:

$$\widehat{\text{GI}} = C_{max} \|\nabla_{\mathbf{a}^{(L)}} \mathcal{L}\|_2. \tag{18}$$

For our method, we use L_2 distance loss function to measure the difference between current student network and the guidance of current teacher:

$$\mathcal{L} = \|S - T\|_2^2. \tag{19}$$

We calculate the first derivative of our loss function:

$$\nabla_{\mathbf{a}^{(L)}} \mathcal{L} = 2 \cdot \|S - T\|_2. \tag{20}$$

According to Eq. (18) and Eq. (20), we set $C_1 = 2C_{max}$, and we define S_0^*/R_i^* is the result that the S_0/R_i has been optimized well:

$$\begin{aligned}
 \widehat{\text{GI}}_{S_0} &= C_1 \|S_0 - T\|_2, \\
 \widehat{\text{GI}}_{S_1} &= C_1 \|R_1 - (T - S_0^*)\|_2, \\
 \widehat{\text{GI}}_{S_2} &= C_1 \|R_2 - (T - S_0^* - R_1^*)\|_2, \\
 &\dots
 \end{aligned} \tag{21}$$

With proper optimization for R_1 , we have the best R_1^* . The best R_1^* is better than other value of R_1 include that R_1 always

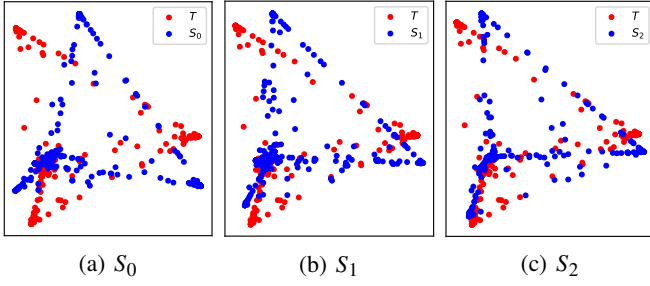


Fig. 7: The visualization of 2D PCA representation of ResKD student's logits using different number of res-students on CIFAR-10. The red dots in (a), (b) and (c) are the distribution of T , ResNet-110, and they are the same one. (a) the distribution of S_0 . (b) the distribution of S_1 . (c) the distribution of S_2 .

equals 0, so we have the upper bound of \widehat{GI}_{S_1} in residual-guided knowledge distillation.

$$\begin{aligned} \widehat{GI}_{S_1} &\leq C_1 \|0 - (T - S_0^*)\|_2 \\ &\leq \widehat{GI}_{S_0}. \end{aligned} \quad (22)$$

We rewrite Eq. (22) and get similar conclusion of other equations, and set $\Delta_i^{(GI)} \geq 0$:

$$\begin{aligned} \widehat{GI}_{S_0} &= \widehat{GI}_{S_1} + \Delta_0^{(GI)}, \\ \widehat{GI}_{S_1} &= \widehat{GI}_{S_2} + \Delta_1^{(GI)}, \\ &\dots, \\ \widehat{GI}_{S_{n-1}} &= \widehat{GI}_{S_n} + \Delta_{n-1}^{(GI)}. \end{aligned} \quad (23)$$

We add all the equations in Eq. (23):

$$\widehat{GI}_{S_0} = \widehat{GI}_{S_n} + \sum_{i=0}^{n-1} \Delta_i^{(GI)}. \quad (24)$$

R_i^* is the best result of optimizing R_i to approach $T - S_0 - \sum_{j=1}^{i-1} R_j$, so we suppose that when we have optimized R_i^* , \widehat{GI}_{S_i} has changed to $k_i(T - S_0 - \sum_{j=1}^{i-1} R_j)$ and $k_i \in (0, 1)$. In this constraint, \widehat{GI}_{S_i} can be rewritten as:

$$\Delta_i^{(GI)} = k_i \cdot \widehat{GI}_{S_{i-1}}, k_i \in (0, 1). \quad (25)$$

When the R_i becomes stronger, the k_i becomes larger and the network R_i bridge the gap better. Also the \widehat{GI}_{S_i} can be rewritten as:

$$\begin{aligned} \widehat{GI}_{S_i} &= \left(\prod_{j=1}^i (1 - k_j) \right) (T - S_0^*), \\ k_j &\in (0, 1). \end{aligned} \quad (26)$$

We can learn that the final performance of S_i is depended on the expression ability of each network in S_0, R_1, \dots, R_n . In Section IV-B1, we will show some results that how the choice of a certain res-student network and the number of res-student networks affect the final performance.

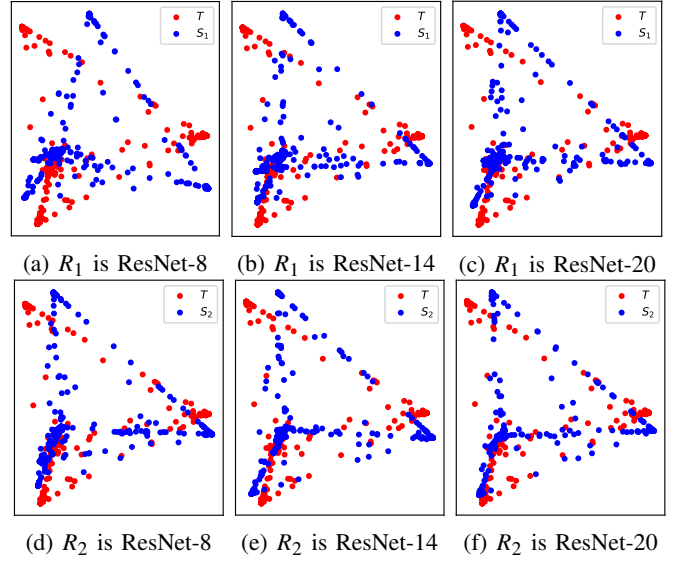


Fig. 8: The visualization of 2D PCA representation of S_1 's / S_2 's logits using different R_1 / R_2 on CIFAR-10. The red dots are the distribution of T , ResNet-110, and they are the same one in (a), (b), (c), (d), (e), and (f). The blue dots in (a), (b), and (c) are the distributions of different S_1 using different R_1 . S_0 is ResNet-20. The blue dots in (d), (e), and (f) are the distributions of S_2 using different R_2 and using ResNet-20 as both S_0 and R_1 .

B. Empirical Analysis

In this part, we show the GI of different students to validate our theoretical analysis on CIFAR-10 first. Next, we show the distribution of logits of different students directly to validate our residual-guided knowledge distillation.

1) *Gap_info (GI) Observation:* We empirically verify whether the expression ability of the student network and res-student networks will influence the GI. The average GI and the average logits distribution samples that anyone of our residual-guided model predicts correctly and S_0 gives the wrong prediction are showed. We use ResNet-110 as the teacher network and ResNet-20 as the S_0 on CIFAR-10. When we focus on R_2 , we set ResNet-20 as R_1 and observe how different res-student network R_2 affects the final performance. The expression of ResX-Y-Z means that we use ResNet-X as S_0 , use ResNet-Y as R_1 and use ResNet-Z as R_2 .

Firstly, we discuss the influence when the number of res-student networks used increases. The results are shown in Table IX. When we use the first res-student network R_1 to bridge the gap between T and S_0 , the output of $S_0 + R_1$ is more similar to the output of T (the average second norm to T is less) and the GI is smaller than the one of S_0 . Similarly, when we use R_2 , the output of $S_0 + R_1 + R_2$ is more likely to T and the GI continues decreasing. When we use ResNet-20 for S_0 , R_1 and R_2 , the GI is about the half of S_0 .

Next, we discuss the difference among different latest res-student networks. In Table IX, the different number of res-student networks can cause different results. When we use ResNet-8 / 14 / 20 to for R_1 , the "GI/ C_1 to T " and " L_2 to T " decrease, and when we use ResNet-20, the value is the

smallest. The phenomenon is similar when we use ResNet-8 / 14 / 20 to for R_2 and fix S_0 and R_1 . We can learn that the stronger R_1/R_2 is, the more similar S_1/S_2 is with the T .

2) *Logits Visualization*: We show the 2D PCA representation of different S_i 's logits on CIFAR-10. In each figure, the red points are the same one and indicate the distribution of T 's logits.

In Fig. 7, the blue points indicate the distributions of S_0 's, S_1 's and S_2 's logits. We use ResNet-20 for S_0 , R_1 and R_2 in this figure. We can learn that with the number of res-students increasing, the distribution of S_i 's logits is more and more similar to the distribution of T 's.

In Fig. 8, the blue points indicate the distribution of S_1 / S_2 . We use ResNet-20 / 14 / 8 for R_1 / R_2 , S_0 is ResNet-20, and R_1 is ResNet-20 when we focus R_2 . We can learn that when res-students R_1 / R_2 is stronger, the distribution of S_1 / S_2 is more similar with the distribution of T .

VI. CONCLUSION

We have studied an under-explored yet important field in knowledge distillation of neural networks. We have shown that using res-students to bridge the gap between student and teacher is a key to improve the quality of knowledge distillation. We propose our residual-guided learning and sample-adaptive inference to realize this idea. We also validate the effectiveness of our approach in various datasets and studied its properties both empirically and theoretically.

REFERENCES

- [1] K. He, X. Zhang, S. Ren, and J. Sun, "Deep residual learning for image recognition," in *Proc. CVPR*, 2016, pp. 770–778.
- [2] G. Huang, Z. Liu, L. Van Der Maaten, and K. Q. Weinberger, "Densely connected convolutional networks," in *Proc. CVPR*, 2017, pp. 4700–4708.
- [3] M. Tan and Q. V. Le, "Efficientnet: Rethinking model scaling for convolutional neural networks," *arXiv preprint arXiv:1905.11946*, 2019.
- [4] H. Touvron, A. Vedaldi, M. Douze, and H. Jégou, "Fixing the train-test resolution discrepancy: Fixefficientnet," *arXiv preprint arXiv:2003.08237*, 2020.
- [5] A. G. Howard, M. Zhu, B. Chen, D. Kalenichenko, W. Wang, T. Weyand, M. Andreetto, and H. Adam, "Mobilenets: Efficient convolutional neural networks for mobile vision applications," *arXiv preprint arXiv:1704.04861*, 2017.
- [6] M. Sandler, A. Howard, M. Zhu, A. Zhmoginov, and L.-C. Chen, "Mobilenetv2: Inverted residuals and linear bottlenecks," in *Proc. CVPR*, 2018, pp. 4510–4520.
- [7] X. Zhang, X. Zhou, M. Lin, and J. Sun, "Shufflenet: An extremely efficient convolutional neural network for mobile devices," in *Proc. CVPR*, 2018, pp. 6848–6856.
- [8] N. Ma, X. Zhang, H.-T. Zheng, and J. Sun, "Shufflenet v2: Practical guidelines for efficient cnn architecture design," in *Proc. ECCV*, 2018, pp. 116–131.
- [9] Y. Zhang, T. Xiang, T. M. Hospedales, and H. Lu, "Deep mutual learning," in *Proc. CVPR*, 2018, pp. 4320–4328.
- [10] T. S. Nowak and J. J. Corso, "Deep net triage: Analyzing the importance of network layers via structural compression," *arXiv preprint arXiv:1801.04651*, 2018.
- [11] E. J. Crowley, G. Gray, and A. J. Storkey, "Moonshine: Distilling with cheap convolutions," in *Proc. NeurIPS*, 2018, pp. 2888–2898.
- [12] H. Wang, H. Zhao, X. Li, and X. Tan, "Progressive blockwise knowledge distillation for neural network acceleration," in *Proc. of IJCAI*, 2018, pp. 2769–2775.
- [13] I.-J. Liu, J. Peng, and A. G. Schwing, "Knowledge flow: Improve upon your teachers," *arXiv preprint arXiv:1904.05878*, 2019.
- [14] J. Gu and V. Tresp, "Search for better students to learn distilled knowledge," *arXiv preprint arXiv:2001.11612*, 2020.
- [15] H. Chen, Y. Wang, C. Xu, Z. Yang, C. Liu, B. Shi, C. Xu, C. Xu, and Q. Tian, "Data-free learning of student networks," in *Proc. ICCV*, 2019, pp. 3514–3522.
- [16] A. Dabouei, S. Soleymani, F. Taherkhani, and N. M. Nasrabadi, "Supernorm: Supervising the mixing data augmentation," *arXiv preprint arXiv:2003.05034*, 2020.
- [17] G. Xu, Z. Liu, X. Li, and C. C. Loy, "Knowledge distillation meets self-supervision," in *Proc. ECCV*. Springer, 2020, pp. 588–604.
- [18] G. Hinton, O. Vinyals, and J. Dean, "Distilling the knowledge in a neural network," *arXiv preprint arXiv:1503.02531*, 2015.
- [19] B. Peng, X. Jin, J. Liu, D. Li, Y. Wu, Y. Liu, S. Zhou, and Z. Zhang, "Correlation congruence for knowledge distillation," in *Proc. ICCV*, 2019, pp. 5007–5016.
- [20] Q. Xie, E. Hovy, M.-T. Luong, and Q. V. Le, "Self-training with noisy student improves imagenet classification," *arXiv preprint arXiv:1911.04252*, 2019.
- [21] J. H. Cho and B. Hariharan, "On the efficacy of knowledge distillation," in *Proc. ICCV*, 2019, pp. 4794–4802.
- [22] J. Gou, B. Yu, S. J. Maybank, and D. Tao, "Knowledge distillation: A survey," *arXiv preprint arXiv:2006.05525*, 2020.
- [23] X.-Y. Zhang, L. Zhang, Z.-Y. Zheng, Y. Liu, J.-W. Bian, and M.-M. Cheng, "Adasample: Adaptive sampling of hard positives for descriptor learning," *arXiv preprint arXiv:1911.12110*, 2019.
- [24] C. Bucilă, R. Caruana, and A. Niculescu-Mizil, "Model compression," in *Proc. of ACM SIGKDD*, 2006, pp. 535–541.
- [25] A. Romero, N. Ballas, S. E. Kahou, A. Chassang, C. Gatta, and Y. Bengio, "FitNets: Hints for thin deep nets," in *Proc. ICLR*, 2015.
- [26] X. Han, X. Song, Y. Yao, X.-S. Xu, and L. Nie, "Neural compatibility modeling with probabilistic knowledge distillation," *IEEE Trans. Image Process.*, vol. 29, pp. 871–882, 2019.
- [27] S. Zagoruyko and N. Komodakis, "Paying more attention to attention: Improving the performance of convolutional neural networks via attention transfer," *arXiv preprint arXiv:1612.03928*, 2016.
- [28] F. Tung and G. Mori, "Similarity-preserving knowledge distillation," in *Proc. ICCV*, 2019, pp. 1365–1374.
- [29] J. Yim, D. Joo, J. Bae, and J. Kim, "A gift from knowledge distillation: Fast optimization, network minimization and transfer learning," in *Proc. CVPR*, 2017, pp. 4133–4141.
- [30] W. Park, D. Kim, Y. Lu, and M. Cho, "Relational knowledge distillation," in *Proc. CVPR*, 2019, pp. 3967–3976.
- [31] L. Yuan, F. E. Tay, G. Li, T. Wang, and J. Feng, "Revisiting knowledge distillation via label smoothing regularization," in *Proc. CVPR*, 2020, pp. 3903–3911.
- [32] S. Ahn, S. X. Hu, A. Damianou, N. D. Lawrence, and Z. Dai, "Variational information distillation for knowledge transfer," in *Proc. CVPR*, 2019, pp. 9163–9171.
- [33] Z. Huang and N. Wang, "Like what you like: Knowledge distill via neuron selectivity transfer," *arXiv preprint arXiv:1707.01219*, 2017.
- [34] N. Passalis and A. Tefas, "Learning deep representations with probabilistic knowledge transfer," in *Proc. ECCV*, 2018, pp. 268–284.
- [35] J. Kim, S. Park, and N. Kwak, "Paraphrasing complex network: Network compression via factor transfer," *arXiv preprint arXiv:1802.04977*, 2018.
- [36] B. Heo, M. Lee, S. Yun, and J. Y. Choi, "Knowledge transfer via distillation of activation boundaries formed by hidden neurons," in *Proc. AAAI*, vol. 33, no. 01, 2019, pp. 3779–3787.
- [37] Y. Tian, D. Krishnan, and P. Isola, "Contrastive representation distillation," *arXiv preprint arXiv:1910.10699*, 2019.
- [38] J. Ba and R. Caruana, "Do deep nets really need to be deep?" in *Proc. NeurIPS*, 2014, pp. 2654–2662.
- [39] B. B. Sau and V. N. Balasubramanian, "Deep model compression: Distilling knowledge from noisy teachers," *arXiv preprint arXiv:1610.09650*, 2016.
- [40] M. Kang, J. Mun, and B. Han, "Towards oracle knowledge distillation with neural architecture search," in *Proc. AAAI*, 2020, pp. 4404–4411.
- [41] S. Ge, S. Zhao, C. Li, Y. Zhang, and J. Li, "Efficient low-resolution face recognition via bridge distillation," *IEEE Trans. Image Process.*, 2020.
- [42] J. Mun, K. Lee, J. Shin, and B. Han, "Learning to specialize with knowledge distillation for visual question answering," Curran Associates Inc., 2018, pp. 8081–8091.
- [43] K. Fu, P. Shi, Y. Song, S. Ge, X. Lu, and J. Li, "Ultrafast video attention prediction with coupled knowledge distillation," in *Proc. AAAI*, 2020, pp. 10 802–10 809.
- [44] J. Li, K. Fu, S. Zhao, and S. Ge, "Spatiotemporal knowledge distillation for efficient estimation of aerial video saliency," *IEEE Trans. Image Process.*, vol. 29, pp. 1902–1914, 2019.

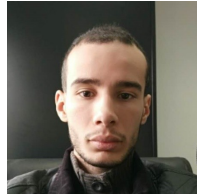
- [45] C. Yang, L. Xie, C. Su, and A. L. Yuille, "Snapshot distillation: Teacher-student optimization in one generation," in *Proc. CVPR*, 2019, pp. 2859–2868.
- [46] S.-I. Mirzadeh, M. Farajtabar, A. Li, N. Levine, A. Matsukawa, and H. Ghasemzadeh, "Improved knowledge distillation via teacher assistant," *arXiv preprint arXiv:1902.03393*, 2019.
- [47] H. Choi, Y. Lee, K. C. Yow, and M. Jeon, "Block change learning for knowledge distillation," *Inf. Sci.*, vol. 513, pp. 360–371, 2020.
- [48] L. K. Hansen and P. Salamon, "Neural network ensembles," *IEEE Trans. Pattern Anal. Mach. Intell.*, vol. 12, no. 10, pp. 993–1001, 1990.
- [49] T. G. Dietterich, "Ensemble methods in machine learning," in *International Workshop on Multiple Classifier Systems*. Springer, 2000, pp. 1–15.
- [50] D. Opitz and R. Maclin, "Popular ensemble methods: An empirical study," *Journal of Artificial Intelligence Research*, vol. 11, pp. 169–198, 1999.
- [51] A. Krogh and J. Vedelsby, "Neural network ensembles, cross validation, and active learning," in *Proc. NeurIPS*, 1995, pp. 231–238.
- [52] J. Xie, B. Xu, and Z. Chuang, "Horizontal and vertical ensemble with deep representation for classification," *arXiv preprint arXiv:1306.2759*, 2013.
- [53] X. Lan, X. Zhu, and S. Gong, "Knowledge distillation by on-the-fly native ensemble," in *Proc. NeurIPS*. Curran Associates Inc., 2018, pp. 7528–7538.
- [54] H. Park and D. Kim, "Acn: Occlusion-tolerant face alignment by attentional combination of heterogeneous regression networks," *Pattern Recognition*, p. 107761, 2020.
- [55] X. Cao, Y. Wei, F. Wen, and J. Sun, "Face alignment by explicit shape regression," *Int. J. Comput. Vis.*, vol. 107, no. 2, pp. 177–190, 2014.
- [56] S. Ren, X. Cao, Y. Wei, and J. Sun, "Face alignment at 3000 fps via regressing local binary features," in *Proc. CVPR*, 2014, pp. 1685–1692.
- [57] X. Zhu, Z. Lei, X. Liu, H. Shi, and S. Z. Li, "Face alignment across large poses: A 3d solution," in *Proc. CVPR*, 2016, pp. 146–155.
- [58] J. Yang, Q. Liu, and K. Zhang, "Stacked hourglass network for robust facial landmark localisation," in *Proc. CVPR Workshop*, 2017, pp. 79–87.
- [59] J. Wan, Z. Lai, J. Liu, J. Zhou, and C. Gao, "Robust face alignment by multi-order high-precision hourglass network," *IEEE Trans. Image Process.*, 2020.
- [60] G. Li, X. Zhang, Z. Wang, Z. Li, and T. Zhang, "Stacnas: Towards stable and consistent optimization for differentiable neural architecture search," *arXiv preprint arXiv:1909.11926*, 2019.
- [61] J. Hu, J. Lu, and Y.-P. Tan, "Deep transfer metric learning," in *Proc. CVPR*, 2015, pp. 325–333.
- [62] Z. Ding and Y. Fu, "Robust transfer metric learning for image classification," *IEEE Trans. Image Process.*, vol. 26, no. 2, pp. 660–670, 2016.
- [63] J. Hu, J. Lu, Y.-P. Tan, and J. Zhou, "Deep transfer metric learning," *IEEE Trans. Image Process.*, vol. 25, no. 12, pp. 5576–5588, 2016.
- [64] A. Katharopoulos and F. Fleuret, "Not all samples are created equal: Deep learning with importance sampling," *arXiv preprint arXiv:1803.00942*, 2018.
- [65] X. Glorot and Y. Bengio, "Understanding the difficulty of training deep feedforward neural networks," in *Proc. AISTATS*, 2010, pp. 249–256.
- [66] S. Ioffe and C. Szegedy, "Batch normalization: Accelerating deep network training by reducing internal covariate shift," *arXiv preprint arXiv:1502.03167*, 2015.
- [67] J. L. Ba, J. R. Kiros, and G. E. Hinton, "Layer normalization," *arXiv preprint arXiv:1607.06450*, 2016.



Xuwei Li received his bachelor of engineering in 2019 from Zhejiang University, China. He is currently a Ph.D. candidate at Zhejiang University. His current research interests include knowledge distillation, image classification and visual relationship detection.



Songyuan Li received his master's degree in 2017 from Zhejiang University, China, where he worked on problems in computer architecture and operating systems. He is currently a Ph.D. candidate at Zhejiang University. His current research interests include knowledge distillation, semantic segmentation and dynamic routing.



Bourahla Omar received the Master's degree from the University of Science and Technology Houari Boumediene, Algiers, Algeria, in 2015. From 2015 until currently (2021), he is pursuing his PhD in Zhejiang University, China. His research interests include machine learning, visual object tracking and rain removal.



Fei Wu received the B.S. degree from Lanzhou University, Lanzhou, Gansu, China, the M.S. degree from Macao University, Taipa, Macau, and the Ph.D. degree from Zhejiang University, Hangzhou, China. He is currently a Full Professor with the College of Computer Science and Technology, Zhejiang University. He was a Visiting Scholar with Prof. B. Yu's Group, University of California, Berkeley, from 2009 to 2010. His current research interests include multimedia retrieval, sparse representation, and machine learning.



Xi Li[†] received the Ph.D. degree from the National Laboratory of Pattern Recognition, Chinese Academy of Sciences, Beijing, China, in 2009. From 2009 to 2010, he was a Post-Doctoral Researcher with CNRS Telecom ParisTech, France. He was a Senior Researcher with the University of Adelaide, Australia. He is currently a Full Professor with Zhejiang University, China. His research interests include visual tracking, compact learning, motion analysis, face recognition, data mining, and image retrieval.